

Citation for published version:
Betts, DN, Kim, HA, Bowen, CR & Inman, DJ 2012, 'Optimal configurations of bistable piezo-composites for energy harvesting', Applied Physics Letters, vol. 100, no. 11, 114104. https://doi.org/10.1063/1.3693523

DOI: 10.1063/1.3693523

Publication date: 2012

Link to publication

Copyright 2012 American Institute of Physics. This article may be downloaded for personal use only. Any other use requires prior permission of the author and the American Institute of Physics.

The following article appeared in Betts, D. N., Kim, H. A., Bowen, C. R. and Inman, D. J., 2012. Optimal configurations of bistable piezo-composites for energy harvesting. Applied Physics Letters, 100 (11), 114104, and may be found at http://dx.doi.org/10.1063/1.3693523

University of Bath

Alternative formats

If you require this document in an alternative format, please contact: openaccess@bath.ac.uk

Copyright and moral rights for the publications made accessible in the public portal are retained by the authors and/or other copyright owners and it is a condition of accessing publications that users recognise and abide by the legal requirements associated with these rights.

Take down policyIf you believe that this document breaches copyright please contact us providing details, and we will remove access to the work immediately and investigate your claim.

Download date: 07 Mar 2023

Optimal configurations of bistable piezo-composites for energy harvesting

D. N. Betts, 1,a) H. A. Kim, 1 C. R. Bowen, 1 and D. J. Inman2

(Received 22 January 2012; accepted 23 February 2012; published online 13 March 2012)

This paper presents an arrangement of bistable composites combined with piezoelectrics for broadband energy harvesting of ambient vibrations. These non-linear devices have improved power generation over conventional resonant systems and can be designed to occupy smaller volumes than magnetic cantilever systems. This paper presents results based on optimization of bistable composites that enables improved electrical power generation by discovering the optimal configurations for harvesting based on the statics of the device. The optimal device aspect ratio, thickness, stacking sequence, and piezoelectric area are considered. Increased electrical output is found for geometries and piezoelectric configurations, which have not been considered previously.

© 2012 American Institute of Physics. [http://dx.doi.org/10.1063/1.3693523]

There has been a recent dramatic increase in the use of wireless sensor networks and electronics using portable energy sources. As a result, energy harvesting methods have been developed¹ to generate electrical energy from ambient vibrations via electrostatic generation, electromagnetic induction,³ and the piezoelectric effect.⁴ Priya⁵ demonstrated that piezoelectrics have several advantages, including ease of integration within a system, higher strain energy densities than electrostatic and electromagnetic systems, and the simplicity of converting strain energy to electrical energy. Vibration based harvesters are often tuned to operate near resonance to maximize their power generation; however, resonant devices are not easily scalable, and performance falls significantly when operated outside their resonant frequencies. This renders linear resonant systems unsuitable for ambient conditions where vibrations generally exhibit multiple time-dependent frequencies. Broadband harvesting can be achieved by exploiting non-linearity in bistable cantilevered beams. Bistability was induced by exciting a ferromagnetic cantilever with two permanent magnets located symmetrically near the free ends.^{7,8} While this system performed effectively over a range of frequencies, it required an obtrusive arrangement of external magnets and can generate unwanted electromagnetic fields. An alternative bistable mechanism has recently been suggested for broadband harvesting—composite laminates with an asymmetric lay-up.4 It is well-known that asymmetry can lead to two stable equilibrium states in thin laminates, leading to large amplitude oscillations between the states when subjected to mechanical vibrations. Arrieta et al. demonstrated high levels of power extraction over a wide frequency range using a bistable laminate $[0_2/90_2]_T$ with four piezoelectric patches to harvest the energy associated with snap-through between stable states. The inherent structural bistability means that an asymmetric laminate can occupy a smaller space and is potentially more convenient and portable. This paper reveals the optimal configurations for a bistable laminate energy harvester offered by the static behavior of the device.

The characterization of the shapes of bistable laminates has been well-established for morphing applications. ^{10–13} A Rayleigh-Ritz formulation of the laminate strain energy minimization is used to characterize the stable shapes. The out-of-plane deflection is approximated by a second order polynomial whose coefficients are typically obtained by numerical techniques. We have derived the exact closed form solution for square orthogonal laminates, ¹³ and this provides a good initial guess for rectangular non-uniform thickness laminates, guaranteeing reliable convergence. This enables iterative optimization of bistable laminates for energy harvesting.

For converting mechanical to electrical energy, four piezoelectric patches are attached to the top surface, each positioned at the centre of one quarter of the laminate surface, Fig. 1. This pattern is mirrored on the bottom surface by

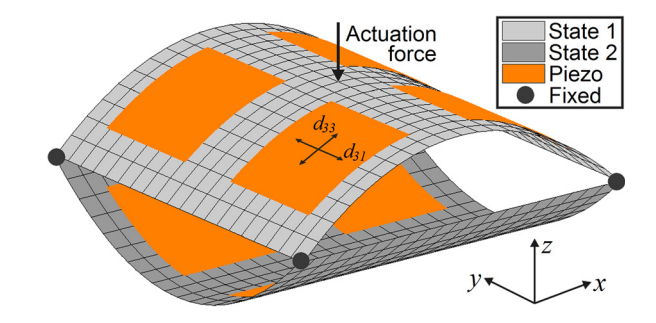


FIG. 1. (Color online) Actuation arrangement for a $[0^P/0_2/90_2/90^P]_T$ laminate with 40% piezoelectric coverage. Superscript P denotes piezo-elements with 0° or 90° poling direction.

¹Department of Mechanical Engineering, University of Bath, Bath BA2 7AY, United Kingdom ²Department of Aerospace Engineering, University of Michigan, Ann Arbor, Michigan 48109, USA

Bistable laminates are of interest for energy harvesting since they provide large structural deformations in response to a relatively small vibrational energy input. Bistability arises from anisotropic thermal expansion during cooling from an elevated cure temperature, leading to a curved deformation. 10 Under certain thermal and geometric conditions, the laminate can have two approximately cylindrical configurations of orthogonal alignment, Fig. 1. It is through the non-linear actuation between the two equilibria that effective broadband energy harvesting is achieved.⁴

a)Electronic mail: D.N.Betts@bath.ac.uk.

piezoelectrics oriented perpendicularly. These piezoelements are treated as anisotropic layers in the same way as the individual laminate plies, with the effect of applied voltage analogous to the temperature change experienced during cure. The laminate is held at all four corners (zero z-displacement) and a displacement applied in the z-direction at the laminate centre to induce a state-change, simulating ambient mechanical motion.

While an increase in piezo-element size increases the area from which electrical energy can be harvested, their additional stiffness reduces the laminate curvature and the resulting stress along the piezoelectric polarization direction, Fig. 2. A high degree of laminate curvature nonlinearly increases the actuation force required to induce snap-through and reduces the overall effectiveness. The energy harvesting characteristics are therefore dependent on piezoelectric area (A), laminate ply thickness (t), ply orientations (θ 's), and device aspect ratio (AR). To determine the correct combination of these parameters for energy harvesting requires an understanding of the complex interactions of the nonlinear behavior.

We now formulate an optimization approach to understand the complex physics of this system where the electrical energy output of the piezo-laminate configuration U is maximized. When operating off-resonance, a piezoelectric layer behaves as a parallel plate capacitor. Hence, the electrical energy generated by snap-through is $^{1}/_{2}CV^{2}$, where C is the piezo-element capacitance and V is the open circuit voltage generated by the direct piezoelectric effect. Under a stress (σ) , the voltage generated is $\sigma g_{ij}t_{p}$, where g_{ij} is the piezoelectric voltage constant (electric field per unit stress), t_{p} is the piezoelectric thickness, and the stresses in x and y are

$$\begin{split} &\sigma_{x} = \bar{Q}_{11}(\varepsilon_{x}^{0} + z\kappa_{x}) + \bar{Q}_{12}(\varepsilon_{y}^{0} + z\kappa_{y}) + \bar{Q}_{16}(\varepsilon_{xy}^{0} + z\kappa_{xy}), \\ &\sigma_{y} = \bar{Q}_{12}(\varepsilon_{x}^{0} + z\kappa_{x}) + \bar{Q}_{22}(\varepsilon_{y}^{0} + z\kappa_{y}) + \bar{Q}_{26}(\varepsilon_{xy}^{0} + z\kappa_{xy}), \end{split}$$

where \bar{Q}_{ij} 's are transformed stiffness terms, ε^0 's are midplane strains, which are small relative to the out-of-plane (z-direction) component, and κ_x , κ_y , and κ_{xy} are the laminate curvatures. Based on the relationship between charge, capacitance, and voltage, the capacitance is equivalent to $d_{ij}\sigma A/V$, where d_{ij} is the piezoelectric strain constant (charge per unit force). We can then characterize the electrical energy based on the static system, $1/2(d_{ij}g_{ij})\sigma^2(At_p)$. When attached to the laminate surface, the piezo-elements are strained in both the poling direction (33 direction, Fig. 1) and transverse direction (31 direction) due to the anticlastic curvatures. The stress varies across the volume of the piezo-elements as a

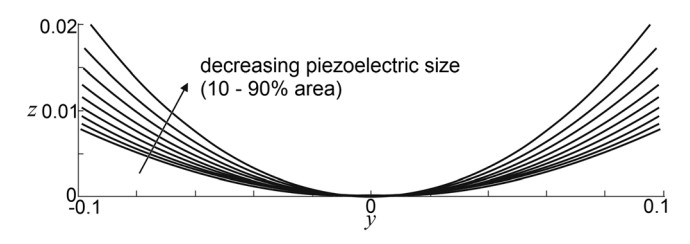


FIG. 2. Major curvature for a square $[0^P/0/90/90^P]_T$ laminate with varying piezoelectric size.

function of the thermally induced strains. The electrical energy for piezo-elements positioned at 0° (top surface) and 90° (bottom surface) is therefore

$$U = 4 \sum_{m=1}^{2} \left[\frac{1}{2} \int_{v_{1}} \left(d_{33} g_{33} \sigma_{x}^{2} + d_{31} g_{31} \sigma_{y}^{2} \right) dv_{1} + \frac{1}{2} \int_{v_{2}} \left(d_{33} g_{33} \sigma_{y}^{2} + d_{31} g_{31} \sigma_{x}^{2} \right) dv_{2} \right],$$

$$(2)$$

where the factor 4 accounts for all piezo-elements on one surface, m defines the associated shape, and v_1 and v_2 are the volumes of two layers on opposite laminate surfaces. The material properties d_{ij} and g_{ij} are considered fixed as their optimum values have been identified by Priya. ¹⁴ The surface area of the laminate is fixed (0.04 m^2) as in Arrieta $et\ al.^4$ A lower bound on t is set as 0.125 mm, consistent with the typical minimum ply thickness. t_p is fixed for practical reasons. All other variables are unbounded. The optimum solutions are subject to constraints to guarantee bistability ¹³ and limiting the piezoelectric strain to below its failure strain $(\sim 2000\ \mu\text{strain})$. The optimization problem is solved using a sequential quadratic programming method with multiple starting points uniformly distributed throughout the design space to capture all optima.

Two optima are found (Table I) with layups $[0^P/0/90/$ 90^{P} _T (global optimum) and $[0^{P}/90/0/90^{P}]_{T}$ (local optimum) where the global solution outperforms the local solution by \sim 65%. In these cases, the major and minor curvatures are aligned with the polarization direction of the piezoelectric to utilise the d_{33} or d_{31} piezoelectric effect, and they are intuitively the optima. The local solution is less optimal due to the reduced curvatures (relative to the global solution) associated with this stacking sequence. What are less obvious are the geometric configurations of piezoelectric area, device aspect ratio, and thickness. These parameters determine the stiffness and actuation behavior of a piezo-laminate and govern the energy generated. The optimum ply thickness is 0.626 mm and 0.619 mm for the global and local solutions, respectively, with significant differences in the piezoelectric areas for the global (72.43%) and local (42.40%) solutions. Despite this significant difference, there is a little variation in the actuation force. A close examination reveals that the optima are highly sensitive to the allowable actuation force, i.e., if the available force is less than 3.39 N, the optimum ply thickness and piezoelectric area change. The strain in both designs is well below the material failure strain, indicating that the optimum designs are unlikely to suffer from mechanical degradation.

TABLE I. Global and local optimum solutions.

	Global	Local
Stacking sequence	[0 ^P /0/90/90 ^P] _T	[0 ^P /90/0/90 ^P] _T
Ply thickness, mm	0.626	0.619
Piezoelectric area, %	72.43	42.40
Aspect ratio	1.0	1.0
Max. strain, μstrain	1097	1113
Snap-through force, N	3.41	3.39
Electrical energy, mJ	33.7	20.4

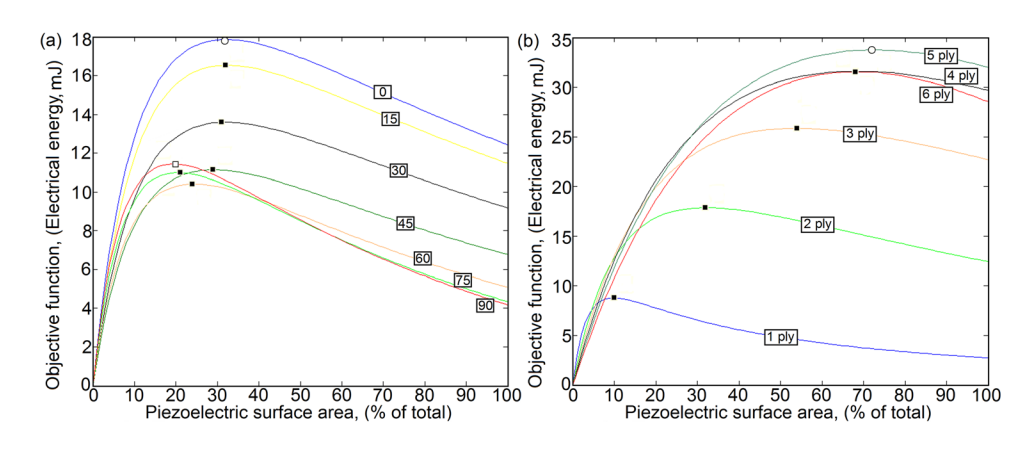


FIG. 3. (Color online) (a) Variation in electrical energy with θ (shown on each line) and piezoelectric surface area for $[0^P/\theta/\theta+90/90^P]_T$ laminates, and (b) variation in electrical energy with $n\times 0.125$ mm plies (shown on each line) and piezoelectric surface area for $[0^P/\theta_n/90^P]_T$ laminates. Black squares mark optima for each θ or n, white circles mark global optima, and white squares mark local optima.

Figure 3(a) shows the energy output for a range of θ values in $[0^P/\theta/\theta+90/90^P]_T$ laminates, 0.2 m edge length, and 0.25 mm ply thickness. The optima for changing θ (black squares) form a convex hull. The maximum electrical energy is observed when θ is 0° corresponding to the global solution (white circle). As θ increases from 0° to 45° , the major laminate curvature reduces, and the alignment of the piezoelectric with laminate curvature becomes less optimal, leading to a decrease in the electrical energy. For θ values from 45° to $\sim 60^{\circ}$, the major curvature continues to decrease, but the piezoelectric alignment improves, the net effect being a more gradual decrease in energy generated. At $\sim 60^{\circ}$, this pattern switches, and the improved alignment of the piezoelectric with curvature becomes dominant compared to the reduced curvature, and the electrical energy increases until the local solution at $\theta = 90^{\circ}$ (white square).

Figure 3(b) shows the effect of varying ply number, n, from 1 to 6 for $[0^P/0_n/90_n/90^P]_T$ laminates. The optima for changing n are marked by black squares. A consistent pattern is observed for n from 1 to 5. The energy generated increases with increasing piezoelectric area to an optimum value with the global optimum at 5 plies (white circle). The optima have larger piezoelectric area as n increases from 1 to 5 since the laminate stiffness increases and the piezoelectric stiffness has less influence on curvature. However, for n = 6, both the optimum area and electrical energy decrease due to the loss of bistability in these stiff laminates (between 6 and 7 plies), leading to significantly reduced curvatures.

Interestingly, square laminates were consistently found to be the optimum, despite the significant out-of-plane deflections achievable by high aspect ratio laminates, Fig. 4.

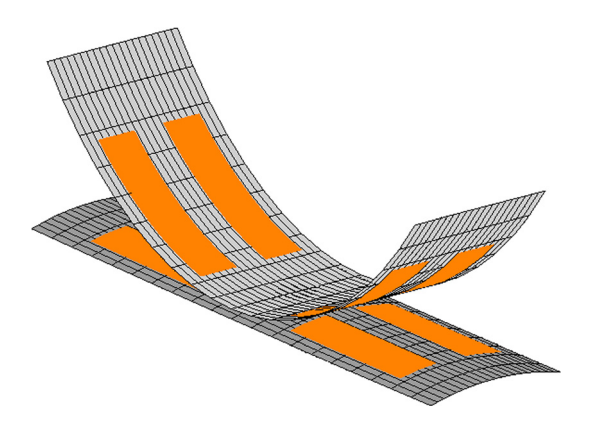


FIG. 4. (Color online) Stable states of a $[0^P/0/90/90^P]_T$ laminate, AR = 3.

For a fixed surface area, the thickness at which bistability is lost decreases with increasing aspect ratio, and since a reduced thickness compromises the energy output (Fig. 3(b)), a low aspect ratio is optimal. The overall sensitivity of objective function to laminate aspect ratio was small since as the laminate size increases, relative to thickness, the curvatures of square and rectangular laminates tend towards the same limiting value. Since the stress in the piezoelectric is directly related to laminate curvature (Eq. (1)), little variation of the objective function is observed.

Although only the static states of the device have been considered here for broadband energy harvesting, the numerous geometric design variables offer flexibility for tailoring to specific resonances. For applications where the device experiences multiple time-dependent frequencies, there may be a balance between reasonable levels of energy harvesting across the entire vibration pattern and tuning the device for optimality close to a single prominent frequency.

This paper has revealed the optimal configurations for a bistable laminate energy harvester. This has been achieved by considering the complex coupling of mechanical and electrical effects, and understanding the underlying science of efficient and high performance bistable energy harvesters. Through variation in ply orientations, laminate geometry, and piezoelectric area, it was found that square cross-ply laminates $[0^P/0/90/90^P]_T$ offer the largest energy outputs since the laminate curvatures are aligned with the piezoelectric polarization axis. A local solution is also found [0^P/90/0/ 90^P]_T with optimal piezoelectric alignment but reduced laminate curvature. Increasing the piezo-element size increases the area from which electrical energy can be harvested; however, their additional stiffness reduces the laminate curvature and stress along the polarization direction. Maximizing the laminate thickness, while maintaining bistability, is observed to improve energy generation and enables larger piezoelements to be used. Aspect ratio is observed to have little or no effect on harvesting metrics. These solutions are found to have optimum ply thicknesses and piezoelectric sizes, which have not been considered in previous scholarly works.

¹S. R Anton and H. A. Sodano, Smart Mater. Struct. 16, R1 (2007).

²P. D. Mitcheson, P. Miao, B. H. Stark, E. M. Yeatman, A. S. Holmes, and T. C. Green, Sens. Actuators A **115**, 523 (2004).

³P. Glynne-Jones, M. J. Tudor, S. P. Beeby, and N. M. White, Sens. Actuators A **110**, 344 (2004).

⁴A. F. Arrieta, P. Hagedorn, A. Erturk, and D. J. Inman, Appl. Phys. Lett. 97, 104102 (2010).

- ⁵S. Priya, J. Electroceram. **19**, 167 (2007).
- ⁶A. Erturk and D. J. Inman, Smart Mater. Struct. **18**, 025009 (2009).
- ⁷A. Erturk, J. Hoffmann, and D. J. Inman, Appl. Phys. Lett. **94**, 254102 (2009)
- ⁸S. C. Stanton, C. C. McGehee, and B. P. Mann, Physica D **239**, 640 (2010)
- ⁹A. F. Arrieta, D. J. Wagg, and S. A. Neild, J. Intell. Mater. Syst. Struct. **22**, 103 (2010).
- ¹⁰M. W. Hyer, **J. Compos. Mater. 15**, 175 (1981).
- ¹¹M. L. Dano and M. W. Hyer, Int. J. Solids Struct. **39**, 175 (2002).
- ¹²D. N. Betts, A. I. T. Salo, C. R. Bowen, and H. A. Kim, Compos. Struct. **92**, 1694 (2010).
- ¹³D. N. Betts, H. A. Kim, and C. R. Bowen, J. Intell. Mater. Syst. Struct. 22, 2181 (2011)
- ¹⁴S. Priya, IEEE Trans. Ultrason. Ferroelectr. Freq. Control **57**, 2610 (2010).
- ¹⁵O. Guillon, F. Thiebaud, and D. Perreux, Int. J. Fract. **117**, 235 (2002).